Triplet Energy Migration among Energetically Disordered Chromophores in Polymer Matrixes. 1. Monte Carlo Simulation for the Hopping of Triplet Excitons

Kenji Hisada,† Shinzaburo Ito, and Masahide Yamamoto*

Department of Polymer Chemistry, Graduate School of Engineering, Kyoto University, Sakyo-ku, Kyoto 606-01, Japan

Received: April 14, 1997; In Final Form: June 18, 1997[⊗]

Triplet energy migration in poly[(9-phenanthrylmethyl methacrylate)-*co*-(methyl methacrylate)] films has been investigated by time-resolved phosphorescence spectroscopy in the temperature range 15−100 K. Phosphorescence spectra from *triplet trap sites* were slightly shifted toward the low-energy side with the elapse of time. The spectral shift was simulated by the Monte Carlo method. The simulation reproduced experimental data, which allowed estimation of the dispersity of the site energies. Due to homogeneous broadening, the distribution function became broader with the increase of temperature.

Introduction

Light-induced processes in aromatic polymers have been well investigated during the past two decades.[1−6] One of the important processes is the excitation energy migration in polymers through the aromatic pendent groups. An electronic excited state initially produced at a donor chromophore by absorption of a photon has been suggested to move to the adjacent donor sites by the Förster or Dexter mechanism.[7,8] The Dexter type energy transfer is often utilized in photosensitive polymers in view of the long lifetime of the triplet state. However, the behavior of triplet energy transfer in polymers has not been fully understood, because of experimental difficulties such as weak emission due to the efficient nonradiative deactivation. The triplet energy migrates by a short-range interaction of chromophores involving the overlap of the electron clouds.[8] This means that the efficient transport of triplet excitons occurs only in concentrated chromophoric systems. In such systems, excited chromophores often form stabilized sites such as an excimer site or a trap site.[9−14]

Previously, the triplet behavior of several kinds of chromophoric polymer films has been reported and the interaction between chromophores classified into two types: excimer-type and trap-type.[15−18] The copolymer film with high concentrations of phenanthrene or naphthalene chromophores shows slightly red-shifted phosphorescence spectra maintaining the vibrational band structure.[16,17] This type of excited species is called a *triplet trap site* (^{3}T*) to distinguish it from the triplet excimer which is often observed in the copolymer films containing carbazole or benzene chromophores.[15,18] The triplet trap sites act as shallow traps for energy migration. The trapped exciton can be thermally released from the trap site, and it migrates through the polymer film with iterative trapping and detrapping processes. The decay profiles of phosphorescence from trap sites are characterized by multiexponential functions or stretched exponential functions. Such decay profiles are observed when the excitons diffuse in the spatially or energetically inhomogeneous matrixes.[19,20]

Many workers have proposed models to describe the complicated relaxation process of excited states.[19−28] Transport properties in inhomogeneous systems are described by a distribution of microscopic (site-to-site) transfer rates (temporal disorder) and by dispersive magnitudes of interactions with the surroundings (energetic disorder). Treatment of the full microscopic problem is an arduous task, which calls for extensive numerical simulations. Spatial randomness may be modeled by fractals,[29,30] and temporal disorder can be accounted for by using a waiting-time distribution, as familiar in continuous-time random walk (CTRW)[31,32] and multiple trapping (MT)[32,33] approaches. A drastic temperature effect on excitation energy migration and trapping could not be explained by both CTRW and MT models. Bässler et al. analyzed the migration process of triplet excitons in organic matrixes by Monte Carlo simulation.[34] They assumed that the distribution of site energies (DOS) is expressed by a Gaussian function and that an exciton hops among these sites. They also reported that this DOS model is adequate for expressing the electron transport, photophysical hole burning, singlet energy migration, and thermally induced transformation of spiropyran in polymer solids.[35,36] Previously, we applied this model to chromophoric polymer systems and successfully represented the phosphorescence decay profiles by this model in the temperature range 115−165 K.[37] In the present study, we observed the spectral shift of phosphorescence for the copolymer films containing phenanthrene chromophores. The spectral shift was simulated by the Monte Carlo method, and the DOS of the triplet states was estimated in the temperature range 15−100 K. The temperature dependence of the energy distribution is also discussed in terms of the thermal fluctuation of the chromophores within the free volume.

Experimental Section

Materials. The synthetic method for poly[(9-phenanthrylmethyl methacrylate)-*co*-(methyl methacrylate)] (P(PhMMA-*co*-MMA)) was as described previously.[16] In the present study, we used two copolymers with various content of 9-phenanthrylmethyl methacrylate (*x*). We abbreviated lower-content copolymer (x = 0.78 mol %) as P(PhMMA-*co*-MMA)L and higer-content one (x = 18.6 mol %) as P(PhMMA-*co*-MMA)H, respectively. 1,4-Dibromonaphthalene (DBN; Tokyo Chemical Industry Co., Ltd.) recrystallized from methanol was used as a triplet energy acceptor. The properties of copolymers and the energy levels of chromophores are listed in Tables 1 and 2, respectively. The energy levels for the lowest singlet state (E_S) of DBN is higher than that of phenanthrene (Ph), i.e., when Ph

† Present address: Department of Applied Chemistry and Biotechnology, Faculty of Engineering, Fukui University, 3-9-1 Bunkyo, Fukui 910, Japan.

⊗ Abstract published in *Advance ACS Abstracts,* August 15, 1997.

S1089-5647(97)01285-6 CCC: $14.00

TABLE 1: Compositions (*x*), Molecular Weights of P(PhMMA-*co*-MMA)s and Chromophore Concentrations ([Ph]), and Average Distances between Phenanthrene Chromophores (*D*) in the Films

sample	*x* (mol %)	M_W[a] (10^5)	[Ph] (mol L^{-1})	*D*[b] (nm)
P(PhMMA-*co*-MMA)L	0.78	1.30	0.09	2.63
P(PhMMA-*co*-MMA)H	18.6	1.20	1.67	1.00

[a] Determined by GPC calibrated with polystyrene standards. [b] Calculated by $D = n^{-(1/3)}$, where *n* is the average number of chromophores per unit volume.

TABLE 2: Singlet and Triplet Energy Levels for Each Chromophore

sample	E_S[a] (kJ mol^{-1})	E_T[a] (kJ mol^{-1})
P(PhMMA-*co*-MMA)L	346	260
DBN	374	237

[a] Calculated from the 0−0 transition band.

is selectively excited at 337 nm, DBN quenches only the lowest triplet state of Ph.

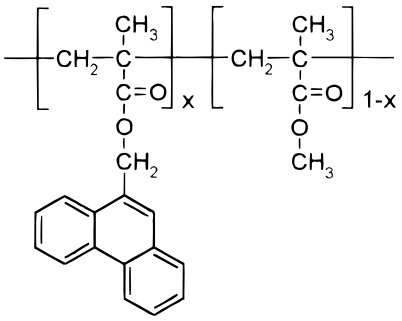

Sample Preparation. A solid film on a quartz plate was formed by casting a solution of the copolymer in a small quantity of 1,2-dichloroethane (spectrophotomeric grade; Dojindo Laboratories). After the solvent evaporated, the film was dried in vacuo for more than 10 h at room temperature and at 110 °C, respectively. In the same manner, DBN doped film was prepared by addition of prescribed amounts of DBN to the casting solution.

Measurements. Steady-state emission spectra were recorded with a Model 850 Hitachi spectrofluorophotometer. Time-resolved phosphorescence spectra and decay curves were measured with a phosphorimeter assembled in our laboratory. A xenon flash lamp (EG&G, FX198UV) and a nitrogen laser (NDC Co., JH-500) were used as the pulsed excitation light source for the measurements in millisecond and in microsecond time regions, respectively. To avoid damage to the detectors by the intense excitation light, a mechanical shutter and a gated photomultiplier (Hamamatsu, R1333) were used. Details of the system have been described elsewhere.[15] The sample temperature was varied by a closed-cycle liquid helium system (Iwatani Plantech Co., CRT 510) consisting of a low-heat-leak helium-transfer line and a cryotip to which a sample holder is attached. Onto the sample holder made of copper the quartz sample plate and its cover plate were placed and fixed with another holed copper block. Indium foil was used between the quartz plates and the copper block to keep efficient thermal conductivity. The film holder is surrounded by a radiation shield and shroud, the interior of which is evacuated during operation. A tip heater was used to counter the cooling action and the temperature was maintained within ±0.1 K by a temperature control unit (Iwatani Plantech Co., TCU-4). A calibrated thermocouple (Au + 0.07% Fe/chromel) was connected to the copper block in the neighborhood of the sample to provide temperature as close to the area of observation as possible.

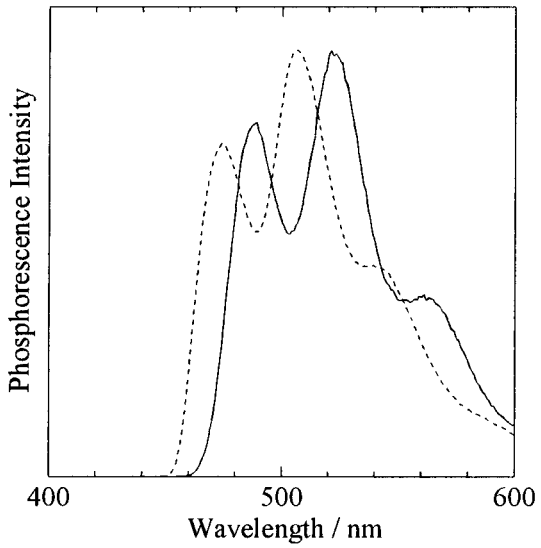

Figure 1. Phosphorescence spectra of P(PhMMA-*co*-MMA)L (- - -) and P(PhMMA-*co*-MMA)H (—) films at 15 K. Spectra are normalized at the maximum of each spectrum peak.

Results and Discussion

Spectroscopic Measurements. Figure 1 shows the phosphorescence spectra for the films of P(PhMMA-*co*-MMA). The 0−0 band of the spectra appeared at 474 nm for the 0.09 mol L^{-1} film (P(PhMMA-*co*-MMA)L) and 489 nm for the 1.67 mol L^{-1} film (P(PhMMA-*co*-MMA)H). In a glassy solution of MTHF, P(PhMMA-*co*-MMA)L gave a phosphorescence spectrum corresponding to the chromophores having no interaction with neighboring chromophores: the 0−0 band of the triplet state of isolated Ph appeared at 461 nm.[16] Hereafter, we will refer to the isolated species as the monomer triplet state (^{3}M*). The spectra of P(PhMMA-*co*-MMA) films were shifted to a longer wavelength with increasing chromophore concentration, but the band shape remained unchanged. Such shifted phosphorescence spectra have been seen in glassy solutions of vinyl polymers bearing pendent aromatic groups.[38−41] The excited triplet state is stabilized by the interactions between chromophores, but the interaction energy is not sufficient to give the spectrum a broad excimeric emission. We will refer to this slightly stabilized state as the trap (^{3}T*) and distinguish it from the excimer which is in a strongly stabilized state.

The temperature dependence of phosphorescence spectra for P(PhMMA-*co*-MMA)H film is shown in Figure 2. The spectra were shifted to a longer wavelength and the intensity decreased with increasing temperature, but the band shape remained the same. This behavior resembles the dependence of the spectra on the chromophore concentration. With elevating temperature, the free volume of the polymer film increases, and the spatial range available for the thermal vibration of the chromophore enlarges. Then, the chromophores can form more stabilized trap sites within their excited lifetime. The broadened spectra at high temperatures may be caused by overlapping of the emission from several trap sites of different energy levels.

Figure 3 shows the typical time-resolved phosphorescence spectra for P(PhMMA-*co*-MMA)H film, which were measured at 100 K. The spectra were gradually shifted to longer wavelengths with the elapse of time. The bandwidth of the spectra became narrower simultaneously with the spectral shift as obviously observed at the 0−0 band. Two reasons are

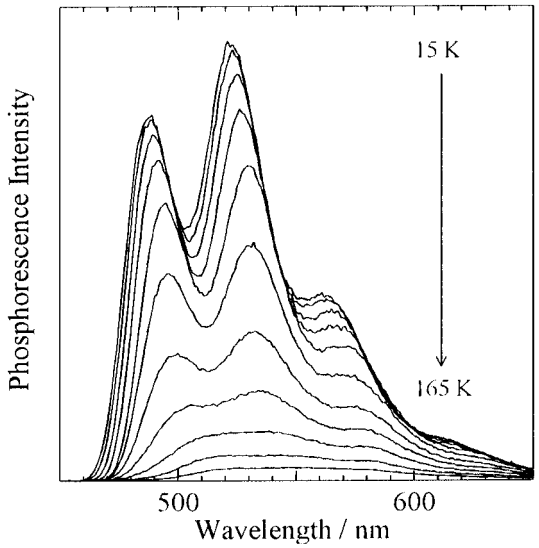

Figure 2. Phosphorescence spectra of P(PhMMA-*co*-MMA)H film. Sample temperature was changed from 15 (top) to 165 K (bottom) by every 15 K separation.

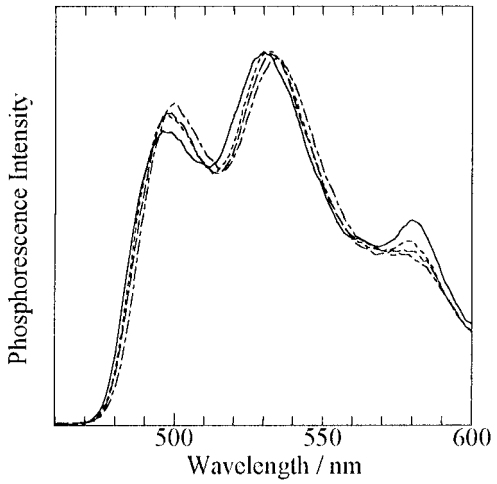

Figure 3. Time-resolved phosphorescence spectra of P(PhMMA-*co*-MMA)H films at 100 K recorded at delay time 0.8 (—), 17 ms (- - -), 33 ms (— — —), and 161 ms (— - —) (sampling time 8 ms). Spectra are normalized at the maximum of each spectrum peak.

considered for this spectral shift. One is the dynamic formation of ^{3}T* site by the motion of the chromophores. The other is the exciton relaxation toward lower energy ^{3}T* sites through the hopping among several trap sites. There is no clear evidence but a support for the latter is provided by the absorption spectra for P(PhMMA-*co*-MMA) film. Figure 4 shows the temperature dependence of the absorption spectra for phenanthrene 0−0 band in P(PhMMA-*co*-MMA)H film. The peak position was maintained constant below 120 K and then shifted toward the lower energy side due to increasing interchromophore interaction. This indicates that the average energy for the Ph singlet state is maintained in the low-temperature range. We assumed that the average energy for ^{3}T* state of the chromophores is also maintained in this temperature range. In an amorphous polymer film, the distribution of the energy of the ^{3}T* sites becomes wider due to inhomogeneity of the environment, like the "*inhomogeneous broadening*" observed in the studies of the spectral hole-burning.[42] The triplet excitons migrate among these broad energy levels and gradually fall in lower energy sites. If the lifetime of the excited states is sufficiently long, the distribution of the triplet excitons finally obeys the Boltzmann relation. The spectral shift in Figure 3 can be interpreted as a result of the relaxation of the triplet excitons.

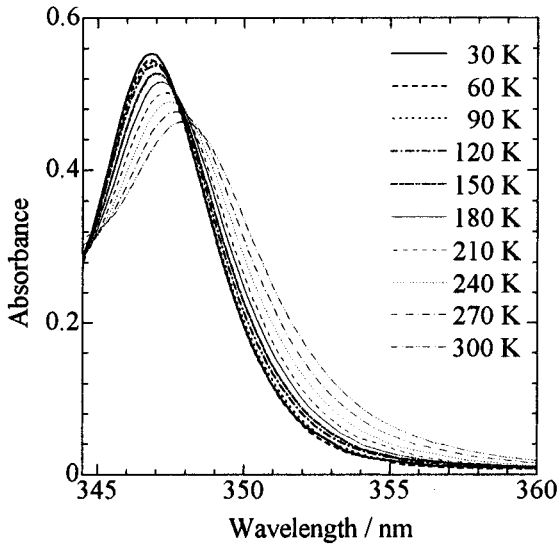

Figure 4. Lowest-energy absorption peak of P(PhMMA-*co*-MMA)H film. Sample temperature was changed from 30 (top) to 300 K (bottom) by every 30 K separation.

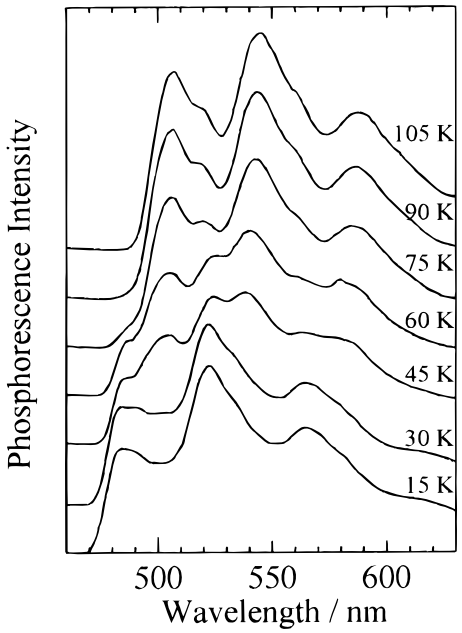

Figure 5. Phosphorescence spectra of the DBN doped P(PhMMA-*co*-MMA)H film at the indicated temperature. The concentration of DBN is 5×10^{-3} mol L^{-1}.

Figure 5 depicts the phosphorescence spectra for P(PhMMA-*co*-MMA)H film containing a small amount of DBN (5×10^{-3} mol L^{-1}). At 15 K, the phosphorescence from only the phenanthrene unit at 485, 522, and 564 nm was observed. With increase in temperature, the Ph phosphorescence decreased, and in place of it, the DBN phosphorescence appeared at 507, 545, and 588 nm. When DBN was doped in P(PhMMA-*co*-MMA)L film, the phosphorescence only from Ph units was observed. This behavior of phosphorescence spectra can be interpreted by the mechanism as shown in Scheme 1.

The migrating exciton is captured by a ^{3}T* site with a potential energy lower than the surrounding sites. At lower temperatures, the triplet exciton cannot overcome the energy barrier so that it is captured immediately and is able to migrate within a narrow range. At higher temperatures, the exciton may overcome the barrier and migrates over a wide range. When acceptors are doped in the film, the probability that the triplet

SCHEME 1: Schematic Illustration of the Energy Migration among the Levels with Broadly Distributed Energies[a]

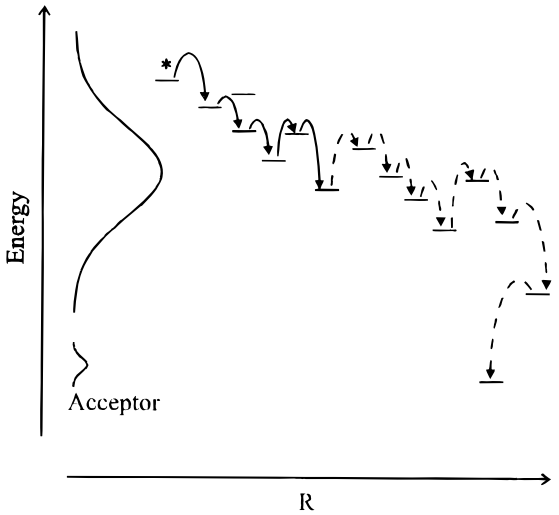

[a] At low temperatures, a exciton (*) is trapped by a shallow ^{3}T* site (→). With increasing temperature, the exciton migrates to deeper ^{3}T* sites (- -→).

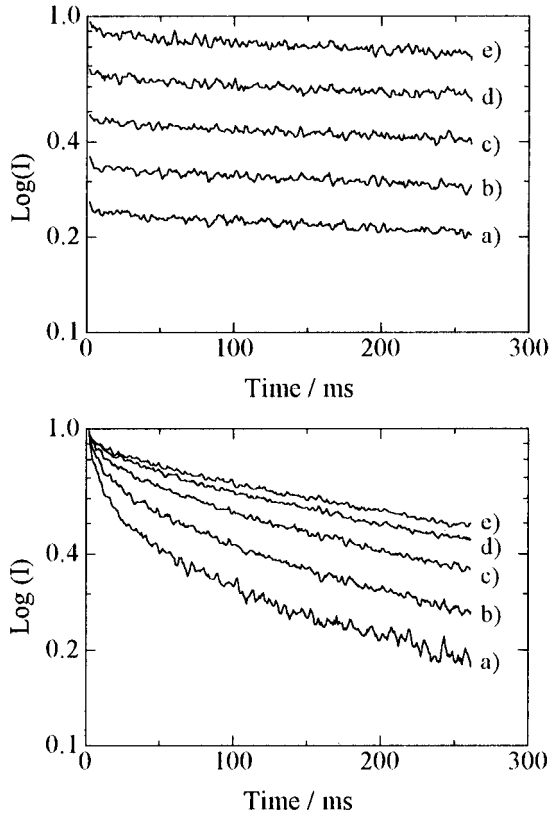

Figure 6. Phosphorescence decay curves of P(PhMMA-*co*-MMA)H at 15 (top) and 100 K (bottom): monitored at (a) 480, (b) 485, (c) 490, (d) 495, and (e) 500 nm.

exciton reaches the acceptor site increases with the temperature. This interpretation is also applicable for the spectral shift in Figure 3.

Phosphorescence decay curves at different temperatures show more direct evidence of this scheme. Figure 6 shows phosphorescence decay curves at different wavelengths. At low temperature (15 K), phosphorescence decay profiles were similar for all wavelengths. At higher temperature (100 K), however, the higher-energy phosphorescence had decayed faster than the lower-energy one.

Assuming that the DOS is a Gaussian for ^{3}T* site of phenanthrene chromophores, very fast internal conversion and intersystem crossing produce a Gaussian distribution of phenanthrene triplet state. The DOS, $f(\epsilon)$, is expressed as follows:

$$f(\epsilon) \propto \exp[-(\epsilon - \langle\epsilon\rangle_0)^2/2\sigma^2] \quad (1)$$

where $\langle\epsilon\rangle_0$ is the average transition energy with respect to the ground state and σ^2 is the site-energy dispersion. The distribution, $g(\epsilon)$, of excitons at $t = 0$ is the same as $f(\epsilon)$: $g_0(\epsilon) = f(\epsilon)$. The distribution of excitons after thermalization is $g_\infty(\epsilon)$ which is expressed by $f(\epsilon)$ weighted by a Boltzmann factor:

$$g_\infty(\epsilon) \propto \exp[-(\epsilon - \langle\epsilon\rangle_0)^2/2\sigma^2]\exp[-(\epsilon - \langle\epsilon\rangle_L)/kT] \quad (2)$$

where $\langle\epsilon\rangle_L$ is the lower limit of the 0−0 transition energy. Equation 2 can be rewritten as a Gaussian form:

$$g_\infty(\epsilon) \propto \exp[-(\epsilon - \langle\epsilon\rangle_\infty)^2/2\sigma^2]\exp[\{2kT(\langle\epsilon\rangle_L - \langle\epsilon\rangle_0) - \sigma^2\}/2k^2T^2]$$
$$\propto \exp[-(\epsilon - \langle\epsilon\rangle_\infty)^2/2\sigma^2] \quad (3)$$

where the averaged energy, $\langle\epsilon\rangle_\infty$, is red-shifted from $\langle\epsilon\rangle_0$ by the amount of $\sigma^2/2kT$. The Gaussian distribution given by eq 1 can be treated as a high-temperature limit ($T \rightarrow \infty$) of eq 3 where no relaxation is involved. At the experimental temperature, T, the distribution function of excitons shifts continuously from the initial Gaussian $f(\epsilon) = g_0(\epsilon)$ toward the final Gaussian $g_\infty(\epsilon)$. Therefore, the transient distribution $g_t(\epsilon)$ during the relaxation process will be also expressed by a Gaussian shape as follows:

$$g_t(\epsilon) \propto \exp[-(\epsilon - \langle\epsilon\rangle_t)^2/2\sigma^2] \quad (4)$$

where the center position $<\epsilon>_t$ and the width σ are both dependent on time. This equation suggests that the mean energy can be monitored by the peak energy of phosphorescence band.

The mean energy of the triplet excitons, $\langle\epsilon\rangle_t$ was estimated from the peak of the second band which is the most intense peak. Time profiles of $\langle\epsilon\rangle_t$ were summarized in Figure 7. For the P(PhMMA-*co*-MMA)L film, $\langle\epsilon\rangle_t$ remained constant in the temperature range 15−100 K. On the other hand, $\langle\epsilon\rangle_t$ for P(PhMMA-*co*-MMA)H film decreased logarithmically with the elapse of time; in particular, it decreased rapidly at the elevated temperatures. If the decrease in $\langle\epsilon\rangle_t$ is caused only by the motion of chromophores, $\langle\epsilon\rangle_t$ should decrease for both polymer films. The different time profiles for the phosphorescence spectra of two polymer films indicate that the spectral shift is due to the triplet energy migration as described above.

Monte Carlo Simulation Method. Bässler et al. analyzed the relaxation processes of electron energy and triplet energy in amorphous organic layers.[36] They assumed that the electron transport and the energy migration in those systems occur through the hopping among the sites which exhibit a Gaussian DOS. Stein et al. used a Voigt DOS to express the absorption bands of chromophores embedded in the glassy matrixes of organic polymers, and those band shapes were in reasonably good agreement with the function.[43] This means that both Lorentzian homogeneous line and the Gaussian inhomogeneous line are good models for the amorphous polymer system. When the homogeneous line width is narrow, a Voigt distribution is similar to a Gaussian one. In this study, we expressed the DOS by a Gaussian function because the observation was performed at low temperatures (15−100 K).

On the basis of these considerations, we simulated the hopping of the triplet excitons among the ^{3}T* sites by the

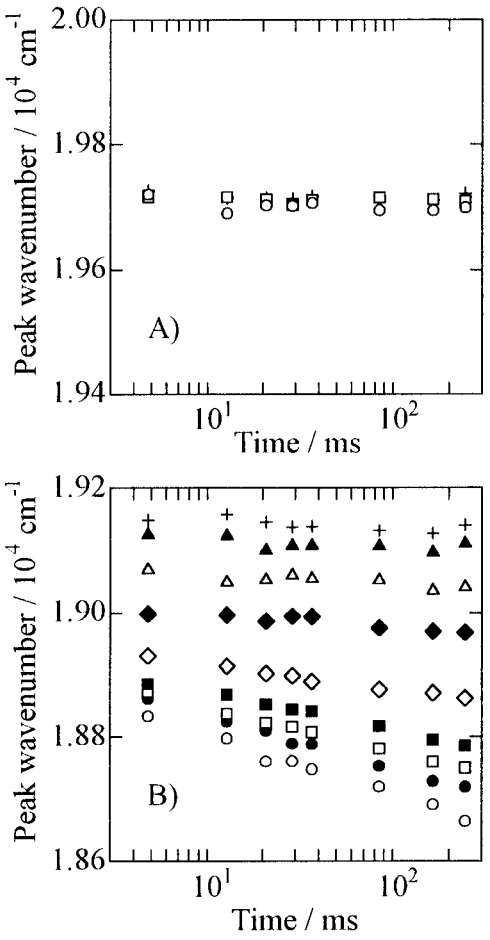

Figure 7. Peak wavenumber of the second phosphorescence band of P(PhMMA-*co*-MMA)L (A) and P(PhMMA-*co*-MMA)H (B) film as a function of delay time at 15 K (+), 30 K (▲), 45 K (△), 60 K (◆), 75 K (◇), 85 K (■), 90 K (□), 95 K (●), and 100 K (○).

following procedure. Figure 8 shows the system in this simulation schematically.

The procedure to set up a specific lattice is as follows. The lattice contains 51 × 51 × 51 = 132 651 sites. The lattice space selected is 1.0 nm which corresponds to the average interchromophore distance in P(PhMMA-*co*-MMA)H film. The origin is placed at the site (25, 25, 25). The site-energy, $f(\epsilon)$, for each of the 132 651 sites is selected at random according to a Gaussian distribution function as eq 5.

$$f(\epsilon)\,\mathrm{d}\epsilon = (2\pi\sigma^2)^{-1/2}\exp[-\epsilon^2/2\sigma^2]\,\mathrm{d}\epsilon \tag{5}$$

A moving particle always started from the center (25, 25, 25). The probability, P_{ij} that the particle makes a jump from (x_i, y_i, z_i) with energy ϵ_i to a site (x_j, y_j, z_j) with energy ϵ_j is

$$P_{ij} = \nu_{ij} / \sum_{l \neq i} \nu_{il} \tag{6}$$

where

$$\nu_{il} = \nu_0 \exp[-2r_{il}/L]\exp[-(\epsilon_l - \epsilon_i)/kT] \tag{7}$$

providing that $\epsilon_l - \epsilon_i \geq 0$.

If $\epsilon_l - \epsilon_i < 0$, then

$$\nu_{il} = \nu_0 \exp[-2r_{il}/L] \tag{8}$$

where ν_0 is constant, r_{il} is the distance between site i and l, and L is a constant called the effective average Bohr radius. Here,

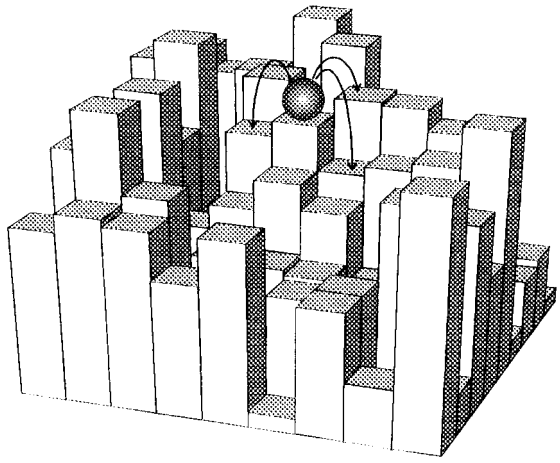

Figure 8. Schematic illustration of a model for the calculation with the Monte Carlo method. A black ball represents the triplet exciton and arrows show the energy migration to adjacent phenanthrene units.

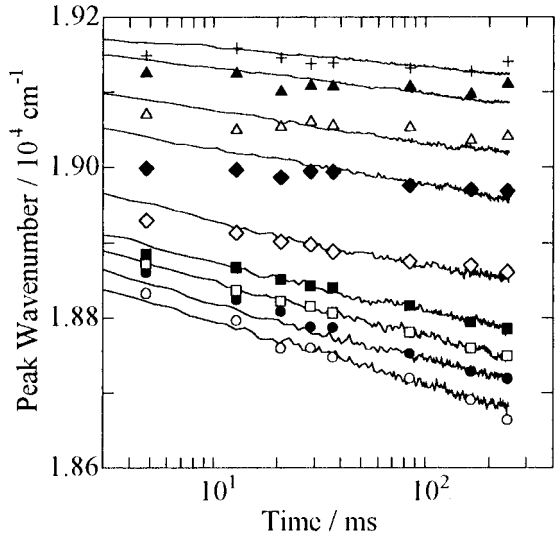

Figure 9. Simulation result for P(PhMMA-*co*-MMA)H film. Gaussian DOS is centered at 19 395 cm^{-1}. Data points are taken from Figure 7B.

$\nu_{il} \neq \nu_{li}$. This is the difference between the spatially disordered system and the energetically disordered one. While the sum over l should include all sites, for practical purpose only the nearest 26 sites are included in the calculation.

A site to which the particle jumps is chosen by a uniform random number n_u according to P_{ij}. The time for the jump, t_{ij}, is determined from

$$t_{ij} = n_{ei} / \sum_{l \neq i} \nu_{il} \tag{9}$$

where n_{ei} is a random number taken from an exponential distribution. The track of the particle is followed and its positions and the site energies are noted as a function of time. These procedure are continued until the time reaches 250 ms. For each configuration, a particle is sent out from the original point and the procedure is repeated 20 times. For a distribution parameter of σ, 300 different random energy configurations were considered. After obtaining the positions and the site energies as a function of time for all the 300 configurations, we obtained the root-mean-square diffusion length, $\langle r(t)^2\rangle^{1/2}$, and the average site energy $\langle\epsilon\rangle_t$.

Figure 9 shows the simulation results for P(PhMMA-*co*-MMA)H film. The calculated lines were in agreement with

TABLE 3: Standard Deviation of the Trap Energy Distribution (σ), Dispersion Parameter (α), and Root-Mean-Square Diffusion Length of Triplet Exciton ($\langle r(t)^2\rangle^{1/2}$) for P(PhMMA-*co*-MMA)H Film

				$\langle r(t)^2\rangle^{1/2}$ (nm)		
temp (K)	σ (cm^{-1})	σ/RT	α^a	2.5 ms	25 ms	250 ms
15	145	13.9	0.076	2.15	2.44	2.87
30	155	7.4	0.23	2.75	3.47	4.32
45	180	5.8	0.33	3.13	4.35	6.64
60	210	5.0	0.39	3.52	5.66	9.47
75	260	5.0	0.39	3.59	5.44	9.31
85	290	4.9	0.40	3.65	5.71	9.85
90	305	4.9	0.40	3.73	5.87	9.74
95	325	4.9	0.40	3.64	5.68	9.88
100	340	4.9	0.40	3.68	5.69	9.97

[a] $\alpha^{-1} = (\sigma/4RT)^2 + 1$.

the experimental values using σ and $\langle\epsilon\rangle_0$ as the fitting parameters. The center of Gaussian DOS could be maintained constant as estimated from absorption spectra. The simulated curves well reproduced the experimental data when the center energy was fixed to 19 395 cm^{-1}. The energy is lower than the average energy of triplet exciton for P(PhMMA-*co*-MMA)L film, 19 763 cm^{-1}, which was obtained from the second peak of the phosphorescence of the film. This means that the triplet state of Ph chromophore is stabilized by the interchromophore interaction for P(PhMMA-*co*-MMA)H film, and the distribution of the triplet energy level shifts toward the lower energy side even at the initial stage, $t = 0$.

The parameters and the results of the simulation are summarized in Table 3. As shown in Table 3, σ is much larger than the thermal energy (RT) in the present temperature range. Thus, the site energy distribution must be a critical factor for the dispersive transport of the triplet excitons. Empirically, the dispersion parameter α was derived as follows,[35]

$$\alpha^{-1} = (\sigma/4RT)^2 + 1 \tag{10}$$

The standard deviation of the trap energy distribution, σ, increased with temperature, but α saturated above 75 K. This means that energetic dispersity is constant between 75 and 100 K. The time profiles of $\langle r(t)^2\rangle^{1/2}$ are also similar in this temperature range. These behaviors are in fair agreement with the previous report that the parameter α well characterizes the transport properties of a hopping system with Gaussian type of energetic disorder.[35] The standard deviation of the trap energy distribution is expressed by the superposition of homogeneous line width ($\Delta\omega_h$) and inhomogeneous line width ($\Delta\omega_i$).[44] The excited-state dephasing interaction and lifetime effect determine $\Delta\omega_h$. The site-energy shift determines $\Delta\omega_i$, which is caused by a small difference in the interaction energy of a chromophore with the environmental matrix. As Stein et al. adopted, the most reasonable function for DOS is the Voigt type which is a Gaussian inhomogeneous line including Lorentzian homogeneous lines for each element. However, we propose to estimate the temperature dependence of DOS profile and its influence to the transport process of the triplet exciton. Thus, we adopted the simplified model that both homogeneous and inhomogeneous lines were expressed by a Gaussian function. By this simplification, σ^2 is obtained from eq 11.

$$\sigma^2 = \Delta\omega_h^{\,2} + \Delta\omega_i^{\,2} \tag{11}$$

In the present study, the spectral shift was simulated at temperatures below the γ-transition of the matrix polymer, which is associated with the rotation of the α-methyl groups of poly(methyl methacrylate). Therefore, $\Delta\omega_i$ is probably constant in the present temperature range. Assuming that $\Delta\omega_h$ follows T^n law, the temperature dependence of σ was fitted by eq 12.

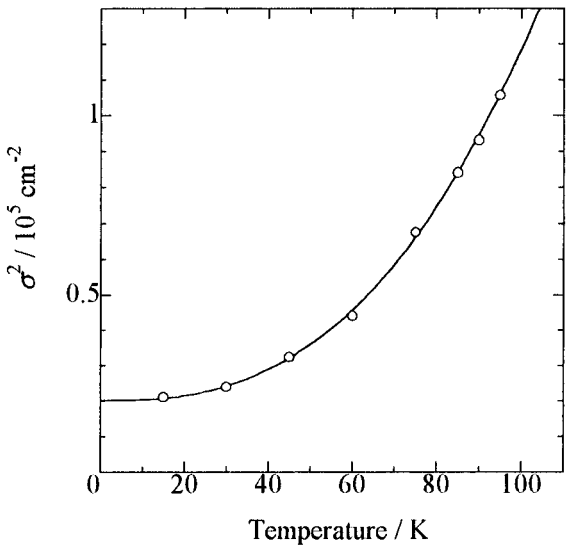

Figure 10. Temperature dependence of the site-energy dispersion, σ^2. The data were fitted by a function: $\sigma^2 = \Delta\omega_h^2 + \Delta\omega_i^2$, where $\Delta\omega_h = aT^n$. $\Delta\omega_h = 0.736 \times T^{1.31}$ cm^{-1}, $\Delta\omega_i = 142$ cm^{-1}.

$$\sigma^2 = (aT^{\,n})^2 + \Delta\omega_i^{\,2} \tag{12}$$

As shown in Figure 10, the relationship of $\Delta\omega_h \propto T^{1.3}$ holds in the temperature range 15−100 K. This relationship has been reported to exist in many amorphous matrixes.[45] Jackson et al. theoretically explained the temperature dependence of the hole width of molecules in soft glasses by considering a combination of two dephasing mechanisms.[46] This similarity reveals that the temperature dependence of σ is mainly attributable to the homogeneous broadening.

Conclusion

Time-resolved phosphorescence spectra were measured for the copolymer films containing Ph moieties. At a high Ph concentration, the phosphorescence spectra were shifted toward the lower energy side. This behavior was explained by the model that the population of the triplet excitons within a Gaussian DOS changes from the uniform distribution toward Boltzmann distribution. The time evolution of the standard deviation of trap energy distribution and the mean value of triplet energies were estimated by a computer simulation. The temperature dependence of the dispersity of DOS is mainly attributed to the homogeneous broadening. At low temperatures, the site energy distribution is one of the critical factors for determining the triplet energy migration.

Acknowledgment. This work was supported by a Grant-in-Aid for Scientific Research on Priority Areas, Photochemical Reactions (No. 06239107) from the Ministry of Education, Science, Sports and Culture of Japan. Computation time was provided by the Supercomputer Laboratory, Institute for Chemical Research, Kyoto University.

References and Notes

(1) (a) Turro, N. J. *Modern Molecular Photochemistry*; Benjamin: Menlo Park, CA, 1978; p 296. (b) Birks, J. B. *Photophysics of Aromatic Molecules*; Wiley: New York, 1970; p 518. (c) Wilkinson, F. *Q. Rev.* **1966**, *20*, 403.

(2) (a) Guillet, J. E. *Polymer Photophysics and Photochemistry*; Cambridge University Press: Cambridge, U.K., 1985. (b) Soutar, I.; Phillips, D. *Photophysical and Photochemical Tools in Polymer Science*; Winnik,

M. A., Ed.; Reidel: Dordrecht, The Netherlands, 1986. (c) Webber, S. C. *Polymer Photophysics*; Phillips, D., Ed.; Chapman and Hall: New York, 1985.

(3) Mort, J., Pfister, G. Eds. *Electronic Properties of Polymers*; John Wiley & Sons: New York, 1982.

(4) Webber, S. E. *Chem. Rev. (Washington, D.C.)* **1990**, *90*, 1469.

(5) Hoyle, C. E.; Torkelson, J. M., Eds. *Photophysics of Polymers; ACS Symposium Series 358*; American Chemical Society: Washington, DC, 1987.

(6) Rabek, J. F. *Mechanisms of Photophysical Processes and Photochemical Reactions in Polymers*; John Wiley & Sons: New York, 1991.

(7) Förster, Th. *Ann. Phys.* **1948**, *2*, 55. Förster, Th.; Kasper, K. *Z. Electrochem.* **1955**, *59*, 976. Förster, Th. *Discuss. Faraday Soc.* **1959**, *27*, 7.

(8) Dexter, D. L. *J. Chem. Phys.* **1953**, *21*, 836.

(9) (a) Hirayama, F. *J. Chem. Phys.* **1965**, *42*, 3163. (b) Zachariasse K.; Kühnle, W. *Z. Phys. Chem. (Munich)* **1976**, *101*, 267.

(10) Nishijima, Y. *J. Polym. Sci. C* **1970**, 31. 353.

(11) Ito, S.; Yamamoto, M.; Nishijima, Y. *Bull. Chem. Soc. Jpn.* **1981**, *54*, 35.

(12) Klöpffer, W.; Fischer, D. *J. Polym. Sci. C* **1973**, *40*, 43.

(13) Gijzeman, O. L. J.; Langelaar, J.; Van Voorst, J. D. W. *Chem. Phys. Lett.* **1970**, *5*, 269.

(14) Itoh, Y.; Webber, S. E. *Macromolecules* **1990**, *23*, 5065.

(15) Ito, S.; Katayama, H.; Yamamoto, M. *Macromolecules* **1988**, *21*, 2456.

(16) Ito, S.; Numata, N.; Katayama, H.; Yamamoto, M. *Macromolecules* **1989**, *22*, 2207.

(17) Katayama, H.; Tawa, T.; Ito, S.; Yamamoto, M. *J. Chem. Soc., Faraday Trans. 2* **1992**, *88*, 2743.

(18) Katayama, H.; Ito, S.; Yamamoto, M. *J. Photopolym. Sci. Technol.* **1991**, *4*, 217.

(19) (a) Yamazaki, I.; Tamai, N.; Yamazaki, T. *J. Phys. Chem.* **1990**, *94*, 516. (b) Tamai, N.; Yamazaki, T.; Yamazaki, I. *Can. J. Phys.* **1990**, *68*, 1013.

(20) Katayama, H.; Tawa, T.; Haggquist, G. W.; Ito, S.; Yamamoto, M. *Macromolecules* **1993**, *26*, 1265.

(21) El-Sayed, F. E.; MacCallum, J. R.; Pomery, P. J.; Shepherd, T. M. *J. Chem. Soc., Faraday Trans. 2* **1979**, *75*, 79.

(22) (a) Zumofen, G.; Blumen, A.; Klafter, J. *J. Chem. Phys.* **1985**, *82*, 3198. (b) Zumofen, G.; Blumen, A.; Klafter, J. *J. Chem. Phys.* **1986**, *84*, 6679.

(23) (a) Lin, Y.; Nelson, M. C.; Hanson, D. M. *J. Chem. Phys.* **1987**, *86*, 1586. (b) Lin, Y.; Dorfman, R. C.; Fayer, M. D. *J. Chem. Phys.* **1989**, *90*, 159.

(24) (a) Byers, J. D.; Friedrichs, M. S.; Friesner, R. A.; Webber, S. E. *Macromolecules* **1988**, *21*, 3402. (b) Byers, J. D.; Parsons, W. S.; Friesner, R. A.; Webber, S. E. *Macromolecules* **1988**, *21*, 3402.

(25) (a) Harmon, L. A.; Kopelman, R. *J. Phys. Chem.* **1990**, *94*, 3454. (b) Li, C. S.; Kopelman, R. *Macromolecules* **1990**, *23*, 2223.

(26) Janse van Rensburg, E. J.; Guillet, J. E.; Whittington, S. G. *Macromolecules* **1989**, *22*, 4212.

(27) Sienicki, K.; Durocher, G. *Macromolecules* **1991**, *24*, 1102.

(28) Kost, S. H.; Breuer, H. D. *Ber. Bunsen-Ges. Phys. Chem.* **1991**, *95*, 480.

(29) Mondelbrot, B. B. *The Fractal Geometry of Nature*; Freeman: San Francisco, 1982).

(30) (a) Blumen, A.; Klafter, J.; Zumofen, G. *Phys. Rev. B* **1983**, *27*, 6112. (b) Klafter, J.; Blumen, A.; Zumofen, G. *J. Stat. Phys.* **1984**, *36*, 561.

(31) Scher, H.; Lax, M., *Phys. Rev. B* **1973**, *7*, 4491. Scher, H.; Lax, M. *Phys. Rev. B* **1973**, *7*, 4502.

(32) Montroll, E. W.; Shlesinger, M. F. In *Non-Equilibrium Phenomena. II. From Stochastics to Hydrodynamics*; Lebowitz, J. L., Montroll, E. W., Eds.; North-Holland: Amsterdam, 1984; p 1.

(33) Shlesinger, M. F.; Montroll, E. W. *Proc. Natl. Acad. Sci. U.S.A.* **1984**, *81*, 1280.

(34) (a) Richert, R.; Ries, B.; Bässler, H. *Philos. Mag. B* **1984**, *49*, L25. (b) Richert, R.; Bässler, H. *J. Chem. Phys.* **1986**, *84*, 3567.

(35) Bässler, H. *Phys. Status Solidi B* **1981**, *107*, 9.

(36) (a) Schönherr, G; Bässler, H.; Silver, M. *Philos. Mag. B* **1981**, *44*, 47. (b) Richert, R.; Elshner, A.; Bässler, H. *Z. Phys. Chem. N.F.* **1986**, *149*, 63.

(37) Katayama, H.; Tawa, T.; Haggquist, G. W.; Ito, S.; Yamamoto, M. *Macromolecules* **1993**, *26*, 1265.

(38) Fox, R. B.; Price, T. R.; Cozzens, R. F.; Echols, W. H. *Macromolecules* **1974**, *7*, 937.

(39) Itaya, A; Okamoto, K; Kusabayashi, S. *Bull. Chem. Soc. Jpn.* **1977**, *50*, 52.

(40) Ito, S.; Nishimoto, S.; Yamamoto, M.; Nishijima, Y. *Rep. Prog. Polym. Phys. Jpn.* **1983**, *26*, 483.

(41) Holden D. A.; Safarzadeh-Amiri, A. *Macromolecules* **1987**, *20*, 1588.

(42) Rebane, K. K.; Rebane, L. A. In *Persistent Spectral Hole-Burning: Science and Applications*; Moerner, W. E., Ed.; Springer-Verlag: Berlin, 1988; Chapter 2.

(43) Stein, A. D.; Peterson, K. A.; Fayer, M. D. *J. Chem. Phys.* **1990**, *92*, 5622.

(44) Moerner, W. E. In *Persistent Spectral Hole-Burning: Science and Applications*; Moerner, W. E., Ed.; Springer-Verlag: Berlin, 1988; Chapter 1.

(45) Thijssen, H. P. H.; van den Berg, R.; Völker, S. *Chem. Phys. Lett.* **1983**, *97*, 295.

(46) Jackson, B.; Silbey, R. *Chem. Phys. Lett.* **1983**, *99*, 331.